The Ries impact, a double layer rampart crater on Earth.

Supplementary material

Macro- and microscopic analyses of Bunte Breccia samples

Intensive macro - and microscopic analyses of several Bunte Breccia samples of two drilling sites (Otting and Itzing) and of surface outcrops revealed that a large amount of water was entrained in the Bunte breccias during flow (***Sup. Fig. s1, s2***). Evidence for fluidized behaviour comes from blocks that are coated with rims of clays in which smaller clastic debris exhibit alignments. This may indicate the presence of water saturated clays that accreted around the blocks during gliding and rolling transport. Evidence also comes from very thin clays with very high aspect ratios that were ductily rolled out. Another indicator is that the vertical vent pipes that occur within the overlying Suevite originate directly from the contact to the Bunte breccias. These pipes likely vented steam from water saturated Bunte Breccia that was covered with hot Suevite (Wittmann and Kenkmann, 2007). Boyce et al. (2012) proposed that martian pits, found in thin ejecta material outside the crater, on terraced blocks in the interior of the crater and on ejecta blankets near the crater rim, were formed due to rapid degassing of water from the pitted material. It is supposed that this process is similar to the degassing of the fall fall-suevite of the Ries impact structure (Boyce et at., 2012, Tornabene et al., 2012).

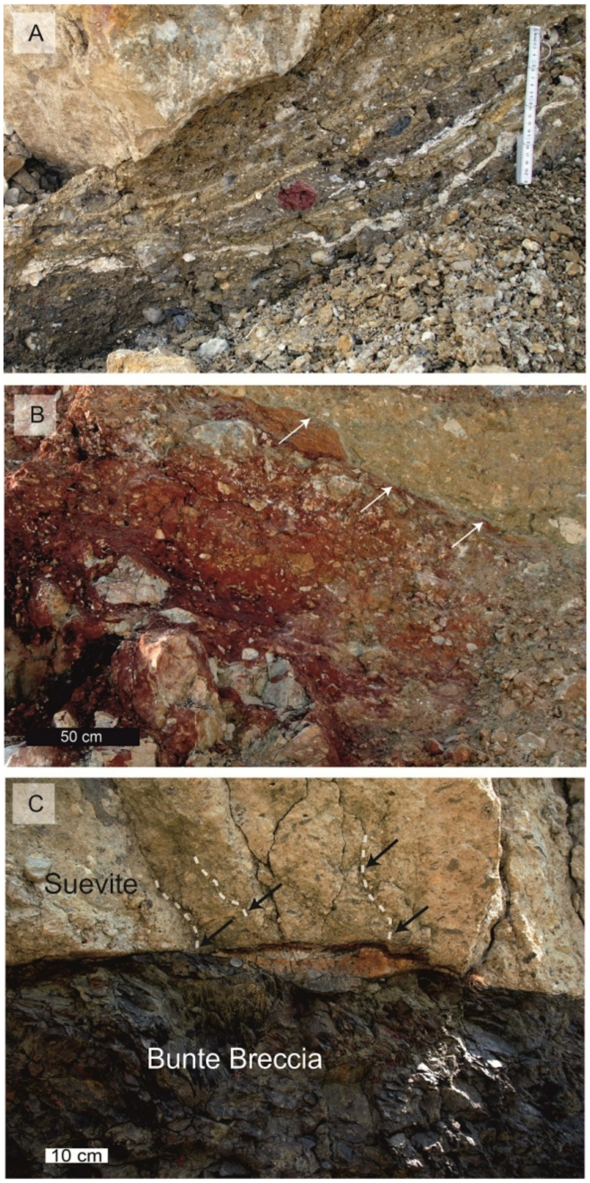

Supplementary Figure s1: Macroscopic fabrics within Bunte Breccia deposits of the continuous ejecta blanket. (a) Gundelsheim, active quarry (GM Gundelsheimer Marmorwerk), 21 km E of crater centre: Variegated clasts are embedded in a clay-rich matrix that displays intensive fluided-assisted ductile flow. The matrix flow led to compositional banding and small-scale disharmonic folding of the matrix. Clasts were mechanically abraded. (b) Mauren-Bräulesberg, active quarry (Märker Zement), 15 km SE of crater centre: two types of matrix-supported breccias are in sharp contact (arrows) to each other. The contact zone is a strongly localized shear plane that developed during the final movements of the Bunte Breccia (c) Aumühle, active quarry (Märker Zement), 9 km NE of crater centre: Sharp contact plane between the Bunte breccia deposits, here represented by dark claystone of Liassic age, and Suevite. Degassing pipes are emanating from the contact plane and penetrate into the hanging wall Suevite deposits (dashed lines). The pipes indicate the presence of water in the Bunte Breccia and subsequent vaporization upon deposition of the hot Suevite.

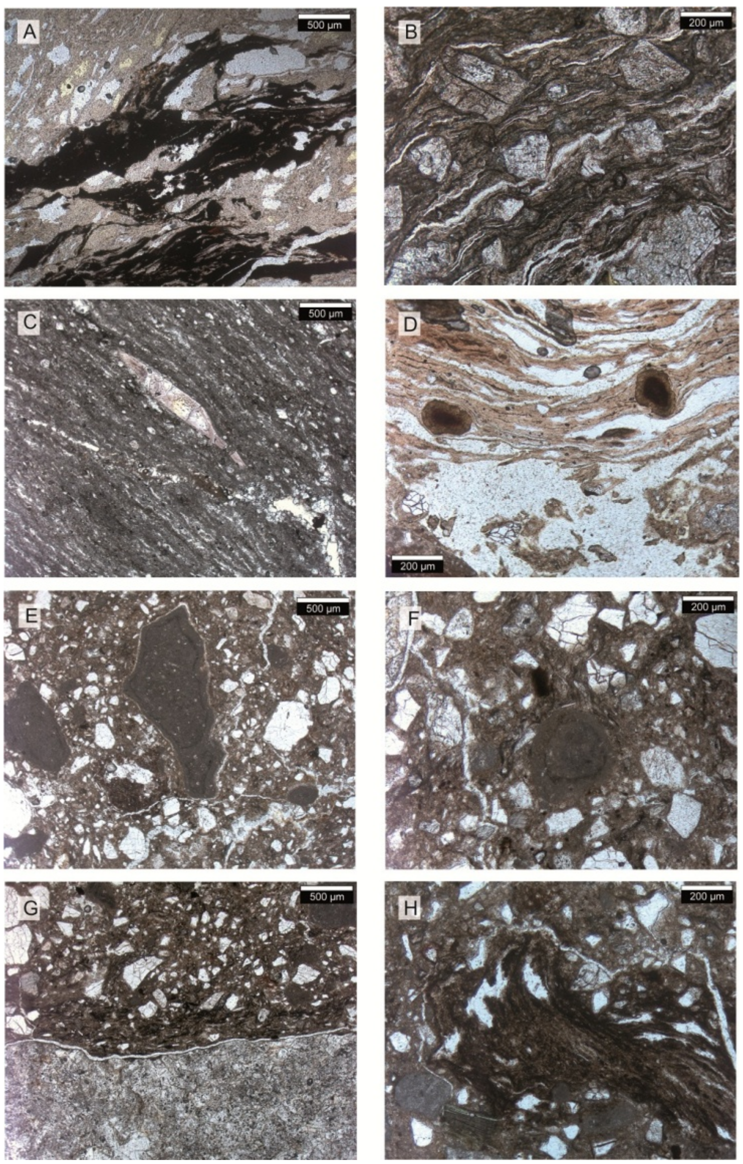

Supplementary Figure s2: Microscopic fabrics within the Bunte Breccia. a-c) drill core Itzing, 20.8 km of the crater centre, d-h) drill core Otting, 17.4 km of the crater centre. a) A ductile flowing limestone-clay-iron-hydroxide assemblage is crosscut by a localized shear plane. B) Clasts of limestone are flowing in a clay-dominated matrix. C) Limestone porphyroclasts are embedded in a fine-grained clay matrix. Porphyroclasts can be used as shear sense indicators (σ-clasts) and suggest simple shear and a laminar low viscosity ductile flow that must have been assisted by a fluid phase. D) Rounded clasts in a ductile lime-clay matrix show a core and mantle structure. E+F) Typical assemblage of sub-angular sedimentary target clasts suspended in Bunte Breccia matrix. The coated clasts in the middle indicate that clays are mantling particles during a rolling process. G) Preferred alignment of particles and flow lines near the contact to a larger limestone clast. H) Breccia in breccias pattern with a chaotic assemblage of ductile deformed and folded clasts in a clay-rich matrix.

ASTER Global Digital Elevation Model – Validation results of GDME 2

			Version 2 - GDME2
Horizontal Error			0.13 arc-sec. to west 0.19 arc-sec. to north
Elevation Error	**Flat and open area (rice farm)**	offset	-0.7 m
		SD	5.9 m
		RMSE	6.1 m
	Mountainous area largely covered by forest	offset	+7.4 m
		SD	12.7 m
		RMSE	15.1 m
Horizontal Resolution			2.4 arc-sec (72m)

Supplementary Table s1: Validation results from a Japanese study of the Global Digital Elevation Model 2 (GDEM2) ASTER dataset that was used for our interpolation study of the ejected Bunte Breccia material (one arc-second corresponds to 30 meters) (modified after Tachikawa et al., 2011).

Interpolation results

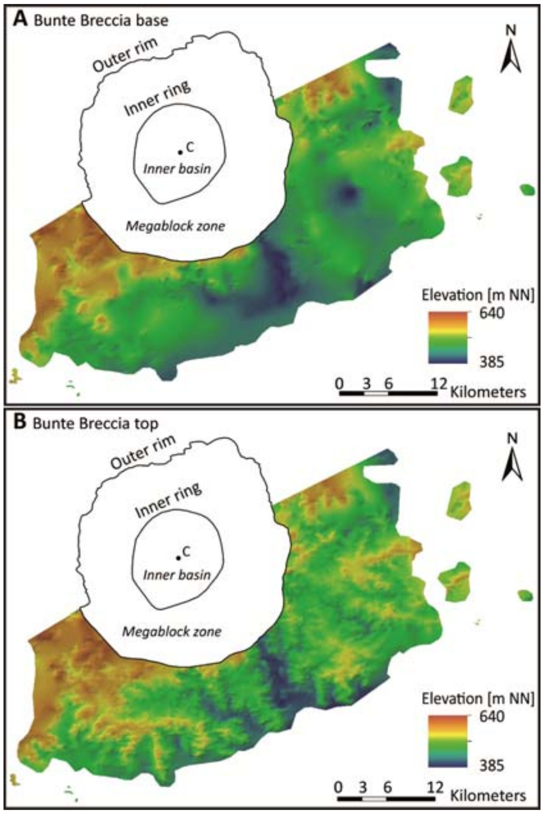

Supplementary Figure s3: Results of the interpolated morphology of the (a) Bunte Breccia base and (b) Bunte Breccia upper surface.

Ejecta layer morphometric parameters

	Average ejecta mobility / crater radius	**Average rampart width [km]**	**Average rampart width / crater radius**
Mars SLE	1.27	1.04	0.17
Mars DLE inner layer	1.37	5.28	**0.66**
Mars DLE outer layer	3.17	1.29	0.17
Mars MLE inner layer	1.25	0.98	0.11
Mars MLE outer layer	2.31	1.13	0.12
GRLE SLE (Nergal)	1.00	0.80	0.20
GRLE DLE inner layer	0.86	8.24	0.43
GRLE DLE outer layer	1.86	4.14	0.12
Earth (Lonar)[*1]	2.34	0.30	0.31
Earth (Ries) inner layer[*2]	1.12	8.70	**0.67**
Earth (Ries) outer layer[*2]	2.36	?	?

Supplementary Table s2: Ejecta layer morphometric parameters for fluidized ejecta craters with ramparts found on Mars, Ganymede (GRLE) and Earth (SLE = single-layer ejecta, DLE = double-layer ejecta, MLE = multiple-layer ejecta) (modified after Boyce et al., 2010; [*1]Maloof et al., 2009; [*2]this study).

Material difference calculation

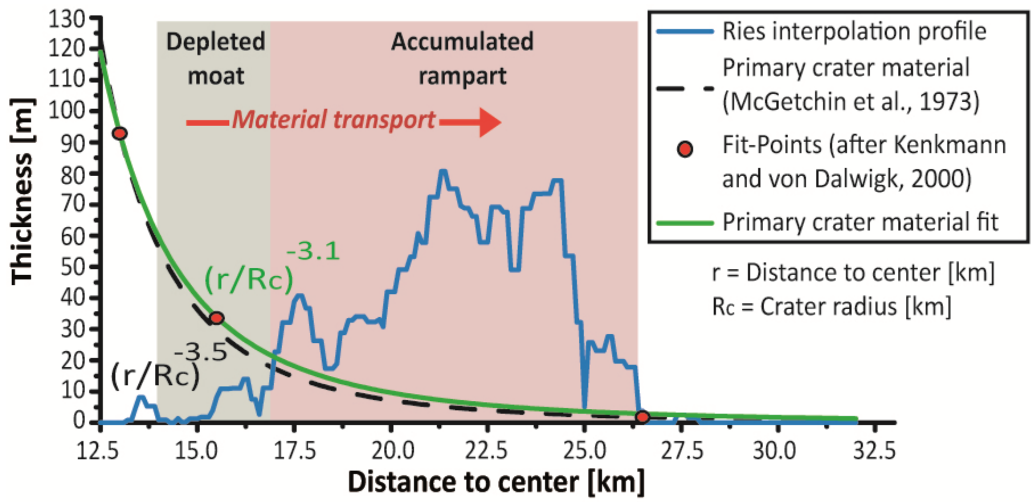

Supplementary Figure s4: Minimum ejecta thickness of one interpolated Bunte Breccia thickness profile (blue line, profile orientation is shown in Fig. 1) of the Ries impact crater compared to the thickness variation of ejected primary crater material (dashed line, calculated after McGetchin et al., 1973) and recalculated and fitted to three fit-points (red dots) after Kenkmann and von Dalwigk (2000) (green line).

References

Boyce, J.M., Barlow, N.G., Mouginis-Mark, P.J., and Stewart, S., 2010, Rampart craters on Ganymede: Their implications for fluidized ejecta emplacement: Meteoritics and Planetary Science, v. 45, no. 4, p. 638–661, doi:10.1111/j.1945-5100.2010.01044.x.

Boyce, J.M., Wilson, L., Mouginis-Mark, P.J., Hamilton, C.W., and Tornabene, L.L., 2012, Origin of small pits in martian impact craters: Icarus, v. 221, p. 262-275, doi:10.1016/j.icarus.2012.07.027.

Kenkmann, T., and von Dalwigk, I., 2000, Radial transpression ridges: A new structural feature of complex impact craters: Meteorics and Planetary Science, v. 35, p. 1189–1201, doi:10.1111/j.1945-5100.2000.tb01508.x.

Maloof, A.C., Stewart, S., Weiss, B., Soule, S., Swanson-Hysell, N., Louzada, K., Garrick, I., and Poussart, P., 2009, Geology of the Lonar Crater: Geological Society of America Bulletin, v. 122, p. 109-126, doi: 10.1130/B26474.1.

McGetchin, T.R., Settle, M., and Head, J.W., 1973, Radial thickness variation in impact crater ejecta: Implications for lunar basin deposits: Earth and Planetary Science Letters, v. 20, p. 226–236, doi:10.1016/0012-821X(73)90162-3.

Tachikawa, T., Kaku, M., Iwasaki, A., Gesch, D., Oimoen, D., Zhang, Z., Danielson. J., Krieger, T., Curtis, B., Haase. J., Abrams, M., Crippen, R., and Carabajal, C., 2011, ASTER Global Digital Elevation Model Version 2 – Summary of Validation Results, METI & NASA, 26pp.

Tornabene, L.L., Osinski, G.R., McEwen, A.S., Boyce, J.M., Bray, V.J., Caudill, C.M., Grant, J.A., Hamilton, C.W., Mattson, S., and Mouginis-Mark, P.J., 2012, Widespread crater-related pitted materials on Mars: Further evidence for the role of target volatiles during the impact process: Icarus, v. 220, p. 348-368, doi: 10.1016/l.icarus.2012.05.022.

Wittmann, A and Kenkmann, T., 2007, Indications for fluidization of the Ries craters´s ejecta blanket. Bridging the gap between nature and modeling II, Montreal.